Microsolvation of Hydrogen Sulfide: Exploration of $H_2S\cdot(H_2O)_n$ and $SH^-\cdot H_3O^+\cdot(H_2O)_{n-1}$ ($n = 5-7$) Cluster Structures on Ab Initio Potential Energy Surfaces by the Scaled Hypersphere Search Method

Satoshi Maeda and Koichi Ohno*

Department of Chemistry, Graduate School of Science, Tohoku University, Aramaki, Aoba-ku, Sendai 980-8578, Japan

Received: October 31, 2007; In Final Form: January 7, 2008

The scaled hypersphere search method was applied to ab initio potential energy surfaces of the $H_2S\cdot(H_2O)_n$/$SH^-\cdot H_3O^+\cdot(H_2O)_{n-1}$ system with $n = 5-7$. Local minima databases including 121, 326, and 553 structures for $n = 5-7$, respectively, were obtained based on calculations at the MP2/6-311++G(3df,2p)//B3LYP/6-31+G** level. In these small cluster sizes, the $SH^-\cdot H_3O^+\cdot(H_2O)_{n-1}$ type is still unstable relative to the $H_2S\cdot(H_2O)_n$ type, and the global minima for $H_2S\cdot(H_2O)_n$ are very similar to those of pure water clusters of $(H_2O)_{n+1}$. Thermodynamic simulations based on the present databases showed a structure transition from the well-mixed $(H_2O)_{n+1}$-like global minimum at low temperatures to unmixed complexes between H_2S and $(H_2O)_n$ at high temperatures.

Introduction

Structures of microsolvated acid molecules have been investigated by many groups,[1−15] and the occurrence of the proton transfer from an acid molecule of AH to H_2O in microsolvation clusters (i.e., $AH\cdot(H_2O)_n \rightarrow A^-\cdot H_3O^+\cdot(H_2O)_{n-1}$) has been discussed. It has been shown that the stability of the $A^-\cdot H_3O^+\cdot(H_2O)_{n-1}$ type depends on two parameters: (1) the number of water molecules and (2) the acidity of the solute. The $A^-\cdot H_3O^+\cdot(H_2O)_{n-1}$ type can be more stable than the $AH\cdot(H_2O)_n$ type with less than five water molecules in cases of strong acid molecules such as HCl[1−3,5,7,9,12] and H_2SO_4,[4,6] while weak acid molecules of HF and H_2S cannot be ionized with a few water molecules.[2,5,8,9,11,12,14] In the case of HF, extensive explorations of cluster structures for $n = 7-10$ were performed by Odde et al. based on high-quality quantum chemical calculations,[14] and it was shown that HF still is not dissociated in these clusters.

There have been a few studies concerning H_2S H-bond cluster systems,[1,2,5,16−28] and the $n = 4$ case,[1,2,5] three structures of the $n = 7$ case,[5] and one type of structure of the $n = 20$ case where H_2S was inserted into a $(H_2O)_{20}$ dodecahedral cage[24] were examined by theoretical calculations concerning the $H_2S\cdot(H_2O)_n$/$SH^-\cdot H_3O^+\cdot(H_2O)_{n-1}$ ($n \geq 2$) system. On the other hand, $H_2S\cdot(H_2O)_n$ is very similar to pure water clusters of $(H_2O)_{n+1}$, where only one oxygen is substituted by the sulfur atom. Since there have been a number of studies concerning small water clusters,[29−40] it may be very interesting to compare the structures and thermodynamic behavior of $H_2S\cdot(H_2O)_n$ with $(H_2O)_{n+1}$. It is well-known that a H-bond via a SH group is much weaker than a H-bond via a OH group and, furthermore, that the van der Waals radius of a S atom is larger than that of an O atom. How such differences influence structures and/or thermodynamic behavior may be determined from the results of extensive search for structures of $H_2S\cdot(H_2O)_n$ clusters.

Here, a search for the most stable structure in terms of free energy at several temperatures is required to study such problems. Analyses of thermodynamic behaviors of H-bond clusters are very difficult, and huge numbers of low-lying local minima will be necessary even for qualitative discussions. Although such explorations have been performed by using MD or Monte Carlo simulations, their applications have been limited to empirical model potentials, in general, due to the large number of potential energy calculations required to achieve sufficient sampling. Unfortunately, there is no reliable model potential that can describe proton-transfer events in the $H_2S\cdot(H_2O)_n$/$SH^-\cdot H_3O^+\cdot(H_2O)_{n-1}$ system correctly, and therefore, one needs to employ quantum mechanical methods such as ab initio calculations and DFT. Obviously, large numbers of energy calculations by such expensive methods are impossible, and geometry optimizations starting from carefully chosen initial structures by intuition and/or experiences have been performed in most of ab initio based computational studies.

Recently, we proposed the use of the anharmonic downward distortion following (ADD-following) algorithm[41−43] as a fully non-empirical approach, concerned with both potential and exploration, for finding many low-lying local minima of H-bond cluster systems.[44] The ADD-following, which can efficiently be performed by the scaled hypersphere search (SHS) method, was originally developed for the exploration of global reaction route networks on potential energy surfaces (PES) via equilibrium structures (EQ) and transition state structures (TS), and its applications to unimolecular systems with 4−12 atoms have successfully located many new EQs and TSs in an automatic way.[45−48] Although we have employed the full ADD-following (FADD-following) method in these unimolecular systems to examine the whole area of the PES including very high-energy regions, the large ADD-following (LADD-following) was introduced for efficient exploration of only low-energy regions of the PES via low-barrier pathways.[44] From many EQs obtained by applications of the LADD-following to ab initio PES,[44,49] we reproduced qualitative features of thermodynamic behavior observed in Monte Carlo simulations[50,51] of $(H_2O)_8$ based on model potentials and recent experiments with different conditions[52−54] of $H^+(H_2O)_8$.

* Corresponding author. Tel.: +81-22-795-6576; fax: +81-22-795-6580; e-mail: ohnok@qpcrkk.chem.tohoku.ac.jp.

10.1021/jp710494n CCC: $40.75
Published on Web 02/29/2008

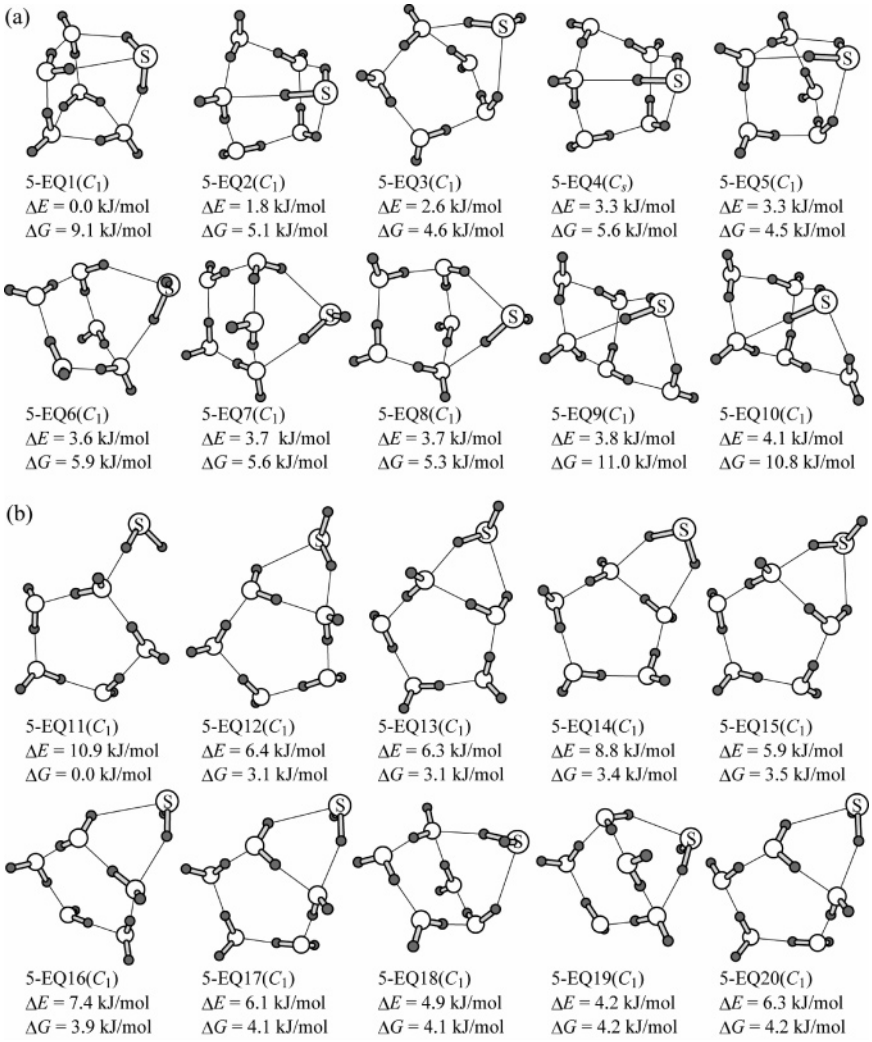

Figure 1. Ten most stable structures of $n = 5$ case in terms of (a) potential energy (ΔE) and (b) free energy at 298.15 K (ΔG). Energies are relative to the most stable structure in kJ/mol. Symmetry is denoted in parentheses.

In this study, we applied this LADD-following to ab initio PESs of the $H_2S\cdot(H_2O)_n/SH^-\cdot H_3O^+\cdot(H_2O)_{n-1}$ system. For $n =$ 5−7, 121, 326, and 553 EQs finally were obtained, respectively, at the MP2/6-311++G(3df,2p)//B3LYP/6-31+G** level. On the basis of this database of EQs, the occurrence of proton transfer from H_2S to H_2O in clusters and the thermodynamic behavior of clusters was also studied.

Materials and Methods

The ADD-following by the SHS Method. The ADD-following was introduced based on insight into the characteristics of potential energy curves of bond breaking and bond reorganization.[41−43] Since typical reaction paths always change their curvatures from concave to convex upon going to a TS or a dissociation channel (DC), slopes should always decline from the respective harmonic curve because of energy lowering interactions leading to a TS or a DC. It follows that such an anharmonic effect (i.e., ADD) can be a symptom of chemical reactions near or around an EQ, and one can determine reaction channels starting from the EQ by following ADD without wandering away from the reaction routes. Directions containing the maximal ADD can be detected by the SHS method as the energy minima on the iso-energy hypersurface of the harmonic potential. Although this hypersurface is a hyperellipsoid when normal coordinates such as Q_i are employed, it can be transformed into a simple hypersphere by using the scaled normal coordinates q_i, where all normal coordinates Q_i are scaled by corresponding eigenvalues λ_i as $q_i = \lambda_i^{1/2}Q_i$. By this transformation, the algorithm of the ADD-following is reduced to energy minimizations on a series of different sizes of scaled hyperspheres with expanding their radii.

We have applied the SHS method to many unimolecular systems with 4−12 atoms,[45−48] and the SHS method has provided many new EQs and TSs in an automatic way. On the basis of these results of the FADD-following where all possible ADDs are followed, we have reported the global reaction route map (GRRM) of each chemical formula. Since applications of the FADD-following to larger systems including more than 20 atoms may not be straightforward, we recently introduced some simplifications to explore quickly the low-energy portions of PES connected via low-barrier pathways.[44] The most important point in this simplification is the use of the LADD-following, in which only large ADDs are followed as important pathways leading to lower energy EQs via low barriers. We reported applications of this LADD-following to ab initio PES of $(H_2O)_8$ and $H^+(H_2O)_8$ clusters,[44,49] and thermodynamic simulations based on these results showed excellent agreement with experimental observations as well as the extensive model potential based Monte Carlo simulations. In this study, we applied this LADD-following to the title system.

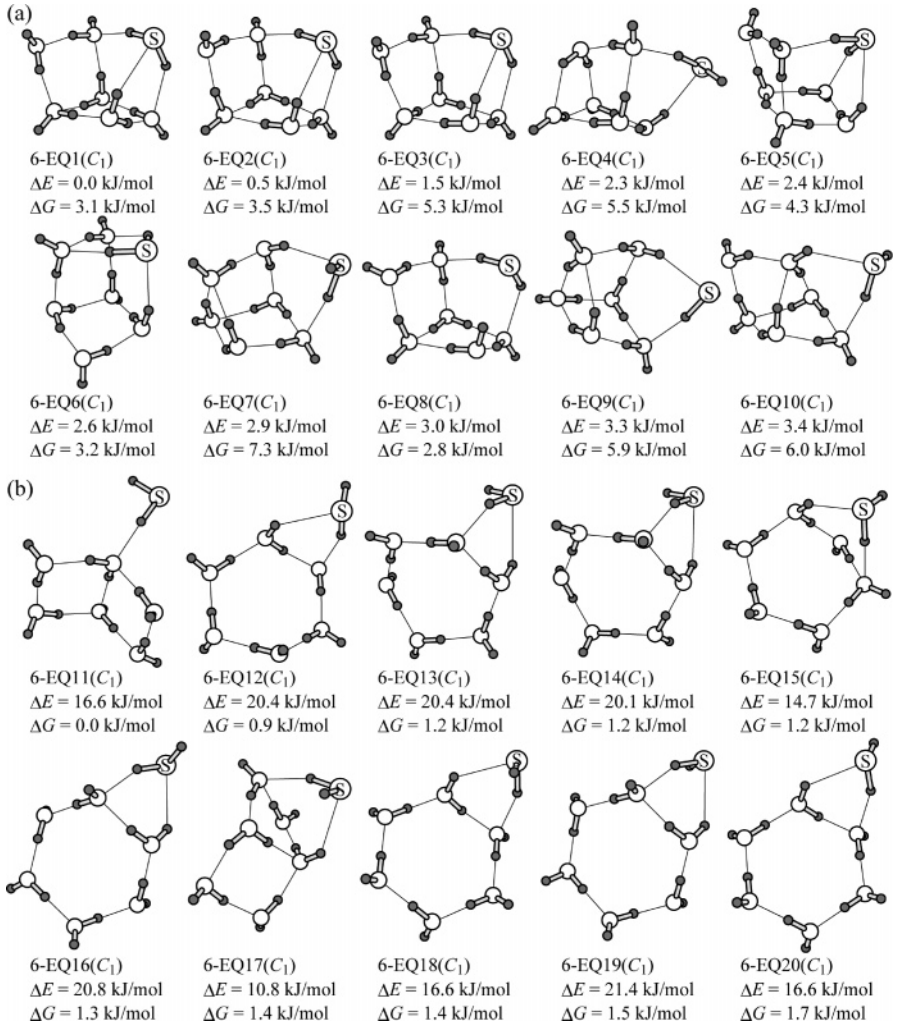

Figure 2. Ten most stable structures of $n = 6$ case in terms of (a) potential energy (ΔE) and (b) free energy at 298.15 K (ΔG). Energies are relative to the most stable structure in kJ/mol. Symmetry is denoted in parentheses.

Computational Details. The SHS method was first applied to the surface at the RHF/3-21G* level. Searches were begun from N (number of atoms) random structures, where H_2O molecules, SH, and H were distributed in a certain ellipsoid with randomization of their center-of-mass position and orientation. Here, 172 369 force calculations and 5340 Hessian calculations for $n = 5$, 415 750 force calculations and 13 153 times Hessian calculations for $n = 6$, and 464 344 force calculations and 14 818 Hessian calculations for $n = 7$ were required. Then, all structures were reoptimized at the B3LYP/6-31+G** level, and vibrational frequencies for zero-point and free energy corrections were also evaluated at this level. Single-point energies were further refined at the MP2/6-311++G(3df,-2p) level. All calculations were made by using a developing version of the GRRM program[41−44] in which energy, gradient, and Hessian values were calculated using the Gaussian 03 program.[55] This choice of the series of ab initio levels was based on our previous applications to $(H_2O)_8$ and $H^+(H_2O)_8$,[44,49] where Hartree−Fock with a double-ζ class basis for initial search, B3LYP with double-ζ plus polarization functions and a diffuse function for the oxygen atom for geometries and harmonic frequencies, and MP2 with a triple-ζ plus diffuse function and many polarization functions for electronic energies was sufficient to reproduce the previous Monte Carlo simulation based thermal behaviors as well as experimental thermal behaviors of such clusters qualitatively.

The populations $P_i(T)$ of the ith EQ at temperature T were calculated by using the superposition approach as[56]

$$P_i(T) = \frac{m_i Z_i(T)}{\sum_k m_k Z_k(T)} \tag{1}$$

where m_i is the number of permutational isomers of the ith EQ,[56] and $Z_i(T)$ is the partition function of the ith EQ at temperature T. The value of $Z_i(T)$ was estimated based on the harmonic approximation for vibrational motion and the rigid rotor approximation for rotational motion.[57] This thermodynamic simulation coupled with the present computation level may cause an error of several tens of degrees Kelvin as discussed in a previous paper,[44] mainly due to the basis set superposition error,[58] lack of dispersion energy in the B3LYP calculations,[59] and anharmonic effects in the vibrational partition function.[60] Therefore, it cannot work even qualitatively when transitions occur very frequently with an interval of several tens of degrees Kelvin. However, the present system is not such a difficult case as can be seen in the following results where transitions take place only one or two times within 0−500 K, and therefore, the present treatment may be used for qualitative discussions of this system.

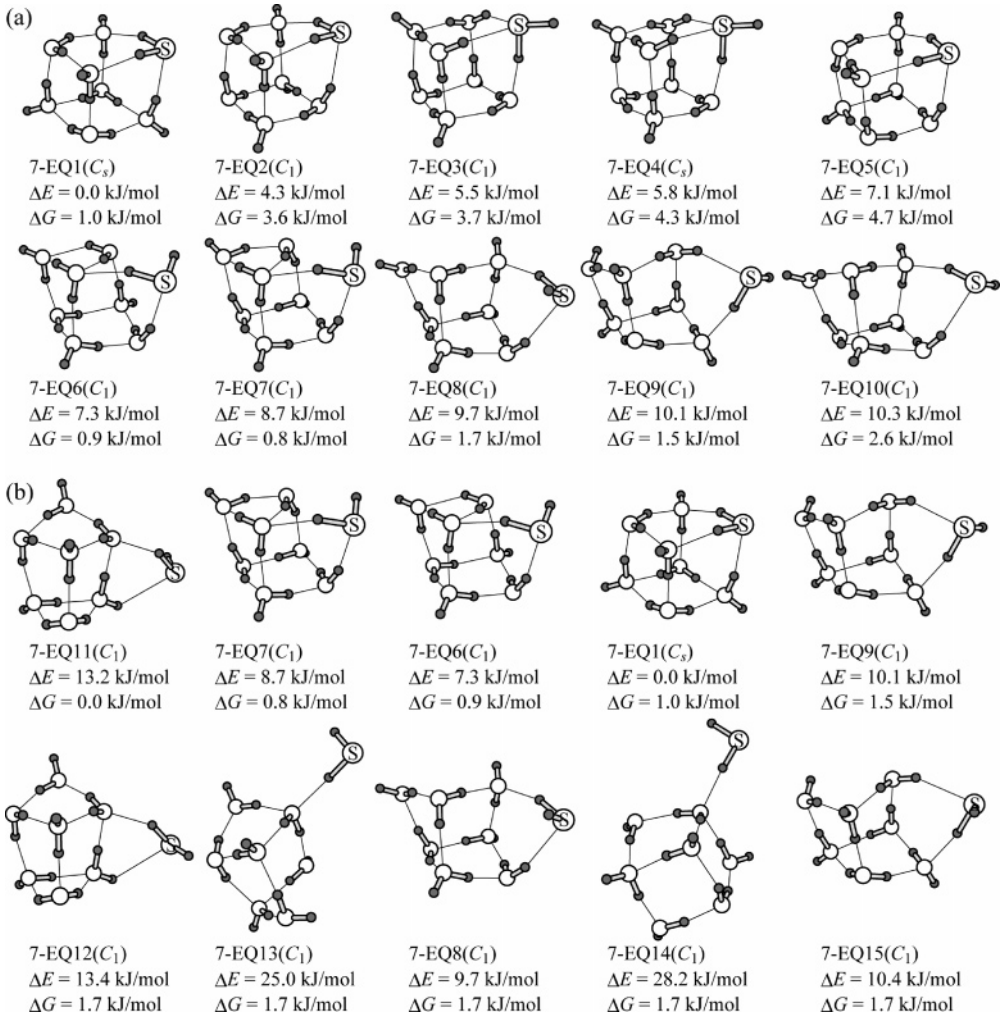

Figure 3. Ten most stable structures of $n = 7$ case in terms of (a) potential energy (ΔE) and (b) free energy at 298.15 K (ΔG). Energies are relative to the most stable structure in kJ/mol. Symmetry is denoted in parentheses.

Results and Discussion

Panel a in Figures 1−3 shows the 10 lowest energy EQs in terms of potential energy among 121, 326, and 553 EQs obtained for $n = 5-7$, respectively. As may be expected, the global minima of each size are very similar to those of the $(H_2O)_{n+1}$ clusters. In the case of $n = 5$, both 5-EQ1 in Figure 1a and the ab initio based global minimum[61−65] of $(H_2O)_6$ are the prism-type structure with nine H-bonds.[66] For $n = 6$, 6-EQ1 in Figure 2a has a form in which a H_2O molecule breaks into an H-bond in 5-EQ1, similar to the relationship between the prism-like global minimum of $(H_2O)_6$ and the global minimum[67] of $(H_2O)_7$. Furthermore, 7-EQ1 in Figure 3a is very similar to the global minimum[68−72,44] of $(H_2O)_8$ with D_{2d} symmetry, and most of the low-lying minima of $H_2S{\cdot}(H_2O)_7$ are cubic structures similar to the $(H_2O)_8$ case. Panel b in Figures 1−3 shows the 10 lowest energy EQs in terms of free energy (at 298.15 K) among 121, 326, and 553 EQs obtained for $n = 5-7$, respectively. As can be seen from Figures 1−3, the lowest-lying EQs in terms of free energy are different from those of potential energy in all of the $n = 5-7$ cases, which implies structural transitions; the thermodynamic behavior will be discussed later. Although only free energy at 298.15 K is considered in Figures 1−3 to show structures after the transition that occurs in the temperature range of 100−200 K, free energy at any temperature can be calculated from electronic energies, structures, and harmonic frequencies listed in the Supporting Information without further ab initio calculations.[57]

Figure 4a−c shows the five lowest energy structures in terms of potential energy among the $SH^-{\cdot}H_3O^+{\cdot}(H_2O)_{n-1}$-type EQs obtained for $n = 5-7$, respectively. Although there have been a few EQs with the Zundel ($H_5O_2^+$) ion core, they have a much higher energy than structures with the Eigen (H_3O^+) core. The most stable $SH^-{\cdot}H_3O^+{\cdot}(H_2O)_{n-1}$-type EQs are less stable than the $H_2S{\cdot}(H_2O)_n$-type EQs in all of the $n = 5-7$ cases. Moreover, thermal entropy effects (at 298.15 K) significantly emphasize the energy difference between the $SH^-{\cdot}H_3O^+{\cdot}(H_2O)_{n-1}$ type and the $H_2S{\cdot}(H_2O)_n$ type because the loss of one SH bond vibrational mode in H_2S ($\sim$2600 cm^{-1}) and simultaneous generation of one OH bond vibrational mode in H_3O^+ ($\sim$3500 cm^{-1}) will increase the total vibrational free energy correction value. Figure 5 depicts the potential energy distributions of the $H_2S{\cdot}(H_2O)_n$ type and the $SH^-{\cdot}H_3O^+{\cdot}(H_2O)_{n-1}$ type for $n = 5-7$, and $SH^-{\cdot}H_3O^+{\cdot}(H_2O)_{n-1}$-type EQs occupy the higher energy region in all panels of Figure 5. It follows that H_2S is still undissociated in clusters with 5−7 water molecules, similar to the HF case.[14] Figure 5 also indicates that the increase in the number of water molecules can dramatically increase the density of the $SH^-{\cdot}H_3O^+{\cdot}(H_2O)_{n-1}$-type local minima and gradually decrease the energy difference between the $H_2S{\cdot}(H_2O)_n$ type and the $SH^-{\cdot}H_3O^+{\cdot}(H_2O)_{n-1}$ type.

To look into the thermodynamic behavior of the present system, we performed simulations via eq 1. Although the simulations were based on all EQs, the $SH^-{\cdot}H_3O^+{\cdot}(H_2O)_{n-1}$ type had nearly no contribution to each result. Panel a in Figures

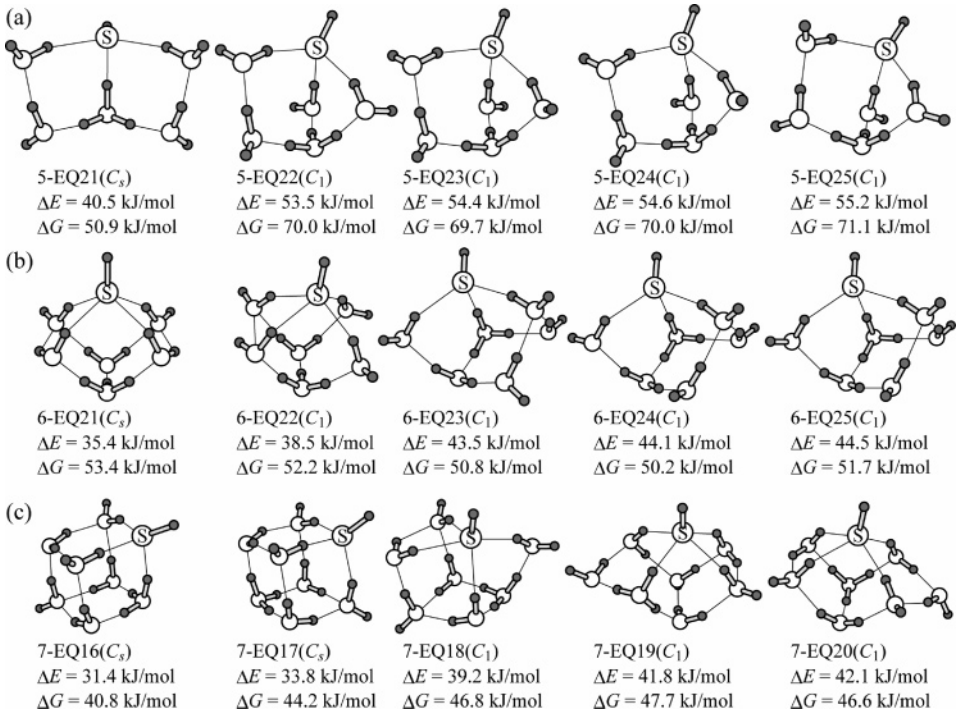

Figure 4. Five most stable structures among $SH^-\cdot H_3O^+\cdot(H_2O)_{n-1}$ types of (a) $n = 5$, (b) $n = 6$, and (c) $n = 7$ cases in terms of potential energy (ΔE). ΔG corresponds to free energy at 298.15 K. Energies are relative to the most stable structure in kJ/mol. Symmetry is denoted in parentheses.

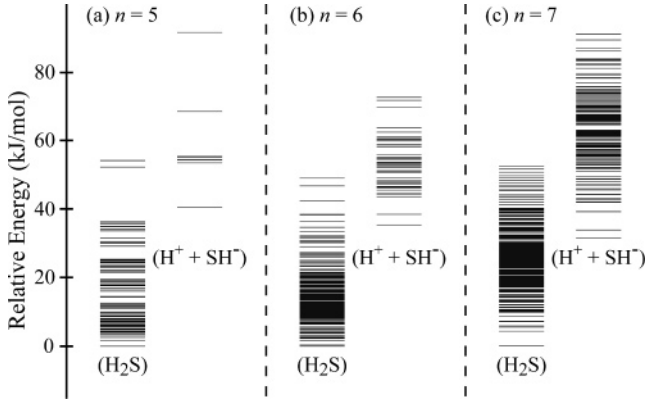

Figure 5. Potential energy distributions of structures of (a) $n = 5$, (b) $n = 6$, and (c) $n = 7$ cases. Energies of neutral clusters of $H_2S\cdot(H_2O)_n$ denoted as (H_2S) and ionized clusters of $SH^-\cdot H_3O^+\cdot(H_2O)_{n-1}$ denoted as ($H^+ + SH^-$) are plotted separately in each panel. Energies are relative to the most stable structure in kJ/mol.

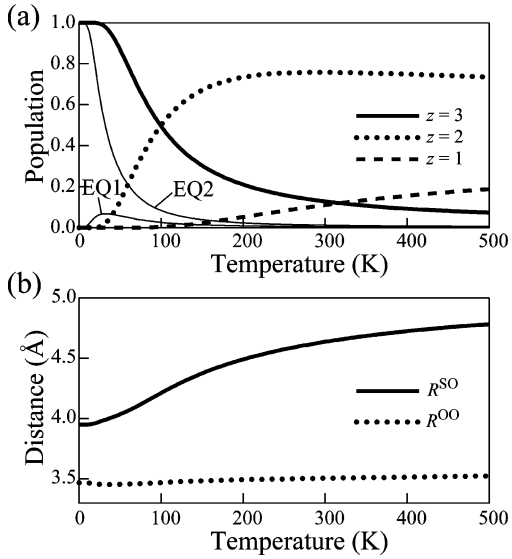

Figure 6. (a) Temperature dependence of population of 5-EQ1, 5-EQ2, and structures with $z = 1-3$ for the $n = 5$ case, where z is the number of hydrogen bonds related to the sulfur atom (the number of O atoms included in the S atom centered sphere with a radius of 4 Å). (b) Temperature dependence of R^{SO} and R^{OO}, where R^{SO} is the average distance between possible pairs of S and O atoms, and R^{OO} is the average distance between possible pairs of two O atoms (see text for further details of R^{SO} and R^{OO}).

6−8 shows the temperature dependence of the sum of populations of EQs with $z = 1-3$, where z is the number of hydrogen bonds related to the sulfur atom (the number of O atoms included in the S-centered sphere with a radius of 4 Å). For example, EQ1, EQ2, EQ4, EQ5, EQ9, and EQ10 are $z = 3$; EQ3, EQ6, EQ7, EQ8, EQ12, EQ13, EQ14, EQ15, EQ16, EQ17, EQ18, EQ19, and EQ20 are $z = 2$; and EQ11 is $z = 1$ in Figure 1. Independent contributions from some EQs are also plotted in these graphs. At low temperatures, populations are dominated by EQs with $z = 3$, which is mostly related to the EQs in panel a of Figures 1−3. As the temperature increases, the curve for $z = 2$ rises and then becomes higher than the $z = 3$ curve. At higher than room temperature, EQs with $z = 1$ also have non-negligible contributions. This trend is common in all sizes of $n = 5-7$, and comparisons between panels a and b in Figures 1−3 indicate that this change from $z = 3$ to $z = 1$ and 2 can be interpreted via structure transitions from well-mixed $(H_2O)_{n+1}$-like structures to just a complex between H_2S and $(H_2O)_n$. To illustrate this point more clearly, we calculated $R^{SO} = \Sigma P_i(T) r_i^{SO}$ and $R^{OO} = \Sigma P_i(T) r_i^{OO}$, which is shown in panel b of Figures 6−8, where $P_i(T)$ is the population of EQi at T calculated by eq 1, r_i^{SO} is the average distance between possible pairs of S and O atoms in EQi, and r_i^{OO} is average distance between possible pairs of two O atoms in EQi. In these graphs, R^{OO} is almost constant over the whole temperature range shown in Figures 6−8, while R^{SO} elongates from ∼4 to ∼5 Å in the temperature range between 100 and 300 K. This clearly shows that H_2S is put out of $(H_2O)_n$, yielding unmixed complexes at high temperatures. This transition can be understood qualitatively from the property of the H-bond via the SH group in

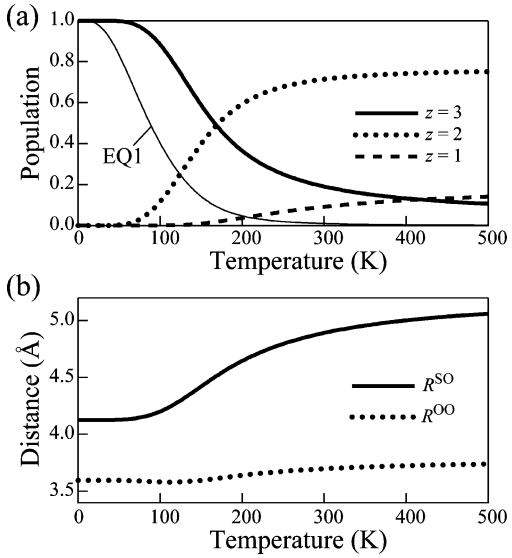

Figure 7. (a) Temperature dependence of population of 6-EQ1 and structures with $z = 1-3$ for the $n = 6$ case, where z is the number of hydrogen bonds related to the sulfur atom (the number of O atoms included in the S atom centered sphere with radius of 4 Å). (b) Temperature dependence of R^{SO} and R^{OO}, where R^{SO} is the average distance between possible pairs of S and O atoms, and R^{OO} is the average distance between possible pairs of two O atoms (see text for further details of R^{SO} and R^{OO}).

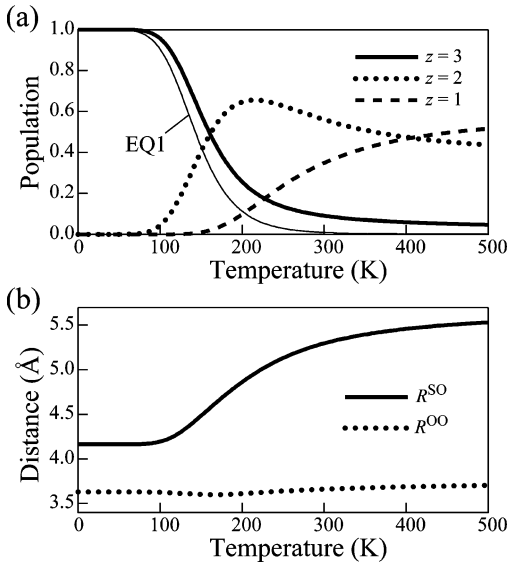

Figure 8. (a) Temperature dependence of population of 7-EQ1 and structures with $z = 1-3$ for the $n = 7$ case, where z is the number of hydrogen bonds related to the sulfur atom (the number of O atoms included in the S atom centered sphere with a radius of 4 Å). (b) Temperature dependence of R^{SO} and R^{OO}, where R^{SO} is the average distance between possible pairs of S and O atoms, and R^{OO} is the average distance between possible pairs of two O atoms (see text for further details of R^{SO} and R^{OO}).

bulk, which is much weaker than the H-bond via the OH group. At low temperatures, a cluster prefers to increase the number of H-bonds to as many as possible even if they are weak, while it is better at high temperatures to gain stabilization energy via vibrational entropy effects rather than maintaining weak undissociated H-bonds.

Conclusion

Ab initio potential energy surfaces of the $H_2S\cdot(H_2O)_n/SH^-\cdot H_3O^+\cdot(H_2O)_{n-1}$ system with $n = 5-7$ were explored by the SHS method. As a result, 121, 326, and 553 local minima could be obtained at the MP2/6-311++G(3df,2p)//B3LYP/6-31+G** level. On the basis of analyses of the present local minima database, we can summarize the nature of the $H_2S\cdot(H_2O)_n/SH^-\cdot H_3O^+\cdot(H_2O)_{n-1}$ system with $n = 5-7$ as follows. H_2S is not solvated in $(H_2O)_n$ within a temperature range of 0−500 K, when the $SH^-\cdot H_3O^+\cdot(H_2O)_{n-1}$-type structure is defined to be a fully solvated structure in the bulk. At low temperatures (<200 K), H_2S is well-mixed with $(H_2O)_n$, with structures very similar to well-characterized $(H_2O)_{n+1}$. At high temperatures (>300 K), H_2S is put out of $(H_2O)_n$, and clusters take forms such as a complex between H_2S and $(H_2O)_n$.

Acknowledgment. S.M. was supported by a Research Fellowship of the Japan Society for Promotion of Science for Young Scientists. Structure reoptimizations at the B3LYP/6-31+G** level and single-point energy refinements at the MP2/6-311++G(3df,2p) level were performed using the parallel computing system in the Tohoku University Information Synergy Center.

Supporting Information Available: List of geometries in the Cartesian representation for 1000 local minimum structures optimized at the B3LYP/6-31+G** level, relative energy values (potential energy with and without the zero-point energy correction and free energy at 298.15 K) at the MP2/6-311++G(3df,2p)//B3LYP/6-31+G** level, and harmonic frequencies at the B3LYP/6-31+G** level. This material is available free of charge via the Internet at http://pubs.acs.org.

References and Notes

(1) Lee, C.; Sosa, C.; Planas, M.; Novoa, J. J. *J. Chem. Phys.* **1996**, *104*, 7081.
(2) Planas, M.; Lee, C.; Novoa, J. J. *J. Phys. Chem.* **1996**, *100*, 16495.
(3) Re, S.; Osamura, Y.; Suzuki, Y.; Schaefer, H. F., III. *J. Chem. Phys.* **1998**, *109*, 973.
(4) Bandy, A. R.; Ianni, J. C. *J. Phys. Chem. A* **1998**, *102*, 6533.
(5) Smith, A.; Vincent, M. A.; Hillier, I. H. *J. Phys. Chem. A* **1999**, *103*, 1132.
(6) Re, S.; Osamura, Y.; Morokuma, K. *J. Phys. Chem. A* **1999**, *103*, 3535.
(7) Milet, A.; Struniewicz, C.; Moszynski, R.; Wormer, P. E. S. *J. Chem. Phys.* **2001**, *115*, 349.
(8) Re, S. *J. Phys. Chem. A* **2001**, *105*, 9725.
(9) Cabaleiro-Lago, E. M.; Hermida-Ramón, J. M.; Rodríguez-Otero, J. *J. Chem. Phys.* **2002**, *117*, 3160.
(10) Chaban, G. M.; Gerber, R. B. *Spectrochim. Acta, Part A* **2002**, *58*, 887.
(11) Kuo, J.-L.; Klein, M. L. *J. Chem. Phys.* **2004**, *120*, 4690.
(12) Odde, S.; Mhin, B. J.; Lee, S.; Lee, H. M.; Kim, K. S. *J. Chem. Phys.* **2004**, *120*, 9524.
(13) Odde, S.; Mhin, B. J.; Lee, H. M.; Kim, K. S. *J. Chem. Phys.* **2004**, *121*, 11083.
(14) Odde, S.; Mhin, B. J.; Lee, K. H.; Lee, H. M.; Tarakeshwar, P.; Kim, K. S. *J. Phys. Chem A* **2006**, *110*, 7918.
(15) Baburao, B.; Visco, D. P., Jr.; Albu, T. V. *J. Phys. Chem. A* **2007**, *111*, 7940.
(16) Kerns, R. C.; Allen, L. C. *J. Am. Chem. Soc.* **1978**, *100*, 6587.
(17) van Hensbergen, B.; Block, R.; Jansen, L. *J. Chem. Phys.* **1982**, *76*, 3161.
(18) Fernández, P. F.; Ortiz, J. V.; Walters, E. A. *J. Chem. Phys.* **1986**, *84*, 1653.
(19) de Oliveira, G.; Dykstra, C. E. *Chem. Phys. Lett.* **1995**, *243*, 158.
(20) Tsujii, H.; Takizawa, K.; Koda, S. *Chem. Phys.* **2001**, *285*, 319.
(21) Bell, A. J.; Wright, T. G. *J. Phys. Chem. A* **2004**, *108*, 10486.
(22) Hermida-Ramón, J. M.; Cabaleiro-Lago, E. M.; Rodríguez-Otero, J. *J. Phys. Chem.* **2005**, *122*, 204315.
(23) Wild, D. A.; Lenzer, T. *Phys. Chem. Chem. Phys.* **2005**, *7*, 3793.
(24) McCarthy, V. N.; Jordan, K. D. *Chem. Phys. Lett.* **2006**, *429*, 166.
(25) Asselin, P.; Soulard, P.; Madebène, B.; Alikhani, M. E.; Lewerenz, M. *Phys. Chem. Chem. Phys.* **2006**, *8*, 1785.
(26) Joshi, R.; Ghanty, T. K.; Naumov, S.; Mukherjee, T. *J. Phys. Chem. A* **2007**, *111*, 2362.

(27) Asselin, P.; Soulard, P.; Madebène, B.; Lewerenz, M. *Phys. Chem. Chem. Phys.* **2007**, *9*, 2868.
(28) Wild, D. A.; Lenzer, T. *Phys. Chem. Chem. Phys.* **2007**, *9*, 5776.
(29) Pribble, R. N.; Zwier, T. S. *Science (Washington, DC, U.S.)* **1994**, *265*, 75.
(30) Liu, K.; Brown, M. G.; Carter, C.; Saykally, R. J.; Gregory, J. K.; Clary, D. C. *Nature (London, U.K.)* **1996**, *381*, 501.
(31) Gregory, J. K.; Clary, D. C.; Liu, K.; Brown, M. G.; Saykally, R. J. *Science (Washington, DC, U.S.)* **1997**, *275*, 814.
(32) Gruenloh, C. J.; Carney, J. R.; Arrington, C. A.; Zwier, T. S.; Fredericks, S. Y.; Jordan, K. D. *Science (Washington, DC, U.S.)* **1997**, *276*, 1678.
(33) Gruenloh, C. J.; Carney, J. R.; Hagemeister, F. C.; Arrington, C. A.; Zwier, T. S.; Fredericks, S. Y.; Wood, J. T., III; Jordan, K. D. *J. Chem. Phys.* **1998**, *109*, 6601.
(34) Buck, U.; Ettischer, I.; Melzer, M.; Buch, V.; Sadlej, J. *Phys. Rev. Lett.* **1998**, *80*, 2578.
(35) Brudermann, J.; Melzer, M.; Buck, U.; Kazimirski, J. K.; Sadlej, J.; Bush, V. *J. Chem. Phys.* **1999**, *110*, 10649.
(36) Gregory, J. K.; Clary, D. C. *J. Phys. Chem.* **1996**, *100*, 18014.
(37) Buck, U.; Huisken, F. *Chem. Rev.* **2000**, *100*, 3863.
(38) Keutsch, F.; Saykally, R. J. *Proc. Natl. Acad. Sci. U.S.A.* **2001**, *98*, 10533.
(39) Ludwig, R. *Angew. Chem., Int. Ed.* **2001**, *40*, 1808.
(40) Keutsch, F. N.; Cruzan, J. D.; Saykally, R. J. *Chem. Rev.* **2003**, *103*, 2533.
(41) Ohno, K.; Maeda, S. *Chem. Phys. Lett.* **2004**, *384*, 277.
(42) Maeda, S.; Ohno, K. *J. Phys. Chem. A* **2005**, *109*, 5742.
(43) Ohno, K.; Maeda, S. *J. Phys. Chem. A* **2006**, *110*, 8933.
(44) Maeda, S.; Ohno, K. *J. Phys. Chem. A* **2007**, *111*, 4527.
(45) Yang, X.; Maeda, S.; Ohno, K. *J. Phys. Chem. A* **2005**, *109*, 7319.
(46) Yang, X.; Maeda, S.; Ohno, K. *Chem. Phys. Lett.* **2006**, *418*, 208.
(47) Yang, X.; Maeda, S.; Ohno, K. *J. Phys. Chem. A* **2007**, *111*, 5099.
(48) Watanabe, Y.; Maeda, S.; Ohno, K. *Chem. Phys. Lett.* **2007**, *447*, 21.
(49) Luo, Y.; Maeda, S.; Ohno, K. *J. Phys. Chem. A* **2007**, *111*, 10732.
(50) Tharrington, A. N.; Jordan, K. D. *J. Phys. Chem. A* **2003**, *107*, 7380.
(51) Miyake, T.; Aida, M. *Chem. Phys. Lett.* **2006**, *427*, 215.
(52) Jiang, J.-C.; Wang, Y.-S.; Chang, H.-C.; Lin, S. H.; Lee, Y. T.; Niedner-Schatteburg, G.; Chang, H.-C. *J. Am. Chem. Soc.* **2000**, *122*, 1398.
(53) Miyazaki, M.; Fujii, A.; Ebata, T.; Mikami, N. *Science (Washington, DC, U.S.)* **2004**, *304*, 1134.
(54) Headrick, J. M.; Diken, E. G.; Walters, R. S.; Hammer, N. I.; Christie, R. A.; Cui, J.; Myshakin, E. M.; Duncan, M. A.; Johnson, M. A.; Jordan, K. D. *Science (Washington, DC, U.S.)* **2005**, *308*, 1765.
(55) Frisch, M. J.; Trucks, G. W.; Schlegel, H. B.; Scuseria, G. E.; Robb, M. A.; Cheeseman, J. R.; Montgomery, J. A., Jr.; Vreven, T.; Kudin, K. N.; Burant, J. C.; Millam, J. M.; Iyengar, S. S.; Tomasi, J.; Barone, V.; Mennucci, B.; Cossi, M.; Scalmani, G.; Rega, N.; Petersson, G. A.; Nakatsuji, H.; Hada, M.; Ehara, M.; Toyota, K.; Fukuda, R.; Hasegawa, J.; Ishida, M.; Nakajima, T.; Honda, Y.; Kitao, O.; Nakai, H.; Klene, M.; Li, X.; Knox, J. E.; Hratchian, H. P.; Cross, J. B.; Adamo, C.; Jaramillo, J.; Gomperts, R.; Stratmann, R. E.; Yazyev, O.; Austin, A. J.; Cammi, R.; Pomelli, C.; Ochterski, J. W.; Ayala, P. Y.; Morokuma, K.; Voth, G. A.; Salvador, P.; Dannenberg, J. J.; Zakrzewski, V. G.; Dapprich, S.; Daniels, A. D.; Strain, M. C.; Farkas, O.; Malick, D. K.; Rabuck, A. D.; Raghavachari, K.; Foresman, J. B.; Ortiz, J. V.; Cui, Q.; Baboul, A. G.; Clifford, S.; Cioslowski, J.; Stefanov, B. B.; Liu, G.; Liashenko, A.; Piskorz, P.; Komaromi, I.; Martin, R. L.; Fox, D. J.; Keith, T.; Al-Laham, M. A.; Peng, C. Y.; Nanayakkara, A.; Challacombe, M.; Gill, P. M. W.; Johnson, B.; Chen, W.; Wong, M. W.; Gonzalez, C.; Pople, J. A. *Gaussian 03, Revision C.02*; Gaussian, Inc.: Pittsburgh, PA, 2004.
(56) Wales, D. J. *Int. Rev. Phys. Chem.* **2006**, *25*, 237.
(57) Jensen, F. *Introduction to Computational Chemistry*; Wiley: Chichester, U.K., 1998.
(58) Boys, S. F.; Bernardi, F. *Mol. Phys.* **1970**, *19*, 553.
(59) Shields, G. C.; Kirschner, K. N. *Synth. React. Inorg. Met.-Org. Nano-Met. Chem.*, in press.
(60) Doye, J. P. K.; Wales, D. J. *J. Chem. Phys.* **1995**, *102*, 9659.
(61) Kim, J.; Kim, K. S. *J. Chem. Phys.* **1998**, *109*, 5886.
(62) Pedulla, J. M.; Kim, K.; Jordan, K. D. *Chem. Phys. Lett.* **1998**, *291*, 78.
(63) Xantheas, S. S.; Burnham, C. J.; Harrison, R. J. *J. Chem. Phys.* **2002**, *116*, 1493.
(64) Losada, M.; Leutwyler, S. *J. Chem. Phys.* **2002**, *117*, 2003.
(65) Dunn, M. E.; Pokon, E. K.; Shields, G. C. *J. Am. Chem. Soc.* **2004**, *126*, 2647.
(66) In the case of $(H_2O)_6$, the cage-type structure is unstable by only 0.1 kcal/mol relative to the prism-type global minimum on the potential energy surface at the MP2 complete basis set limit (see ref 63), and the cage-type structure is more stable when zero-point energy is taken into account by high-level ab initio theory (see ref 61) in agreement with the experimental observation of the cage-type structure (see ref 30).
(67) Kim, J.; Majumdar, D.; Lee, H. M.; Kim, K. S. *J. Chem. Phys.* **1999**, *110*, 9128.
(68) Kim, K. S.; Dupuis, M.; Lie, G. C.; Clementi, E. *Chem. Phys. Lett.* **1986**, *131*, 451.
(69) Kim, J.; Mhin, B. J.; Lee, S. J.; Kim, K. S. *Chem. Phys. Lett.* **1994**, *219*, 243.
(70) Lee, H. M.; Suh, S. B.; Lee, J. Y.; Tarakeshwar, P.; Kim, K. S. *J. Chem. Phys.* **2000**, *112*, 9759.
(71) Xantheas, S. S.; Aprà, E. *J. Chem. Phys.* **2004**, *120*, 823.
(72) Day, M. B.; Kirschner, K. N.; Shields, G. C. *Int. J. Quantum Chem.* **2005**, *102*, 565.